WORLD JOURNAL OF PHARMACEUTICAL RESEARCH
Coden USA: WJPRAP Impact Factor 8.63
Volume 15, Issue 15, 1950-1964. Research Article ISSN 2277–7105

COMPUTATIONAL STUDY ON RNA DINUCLEOTIDES USING THE AM1 SEMI-EMPIRICAL METHOD

Bojja Rajeshwar Rao*

Senior Chemist (Retired), Chemical Division, Kakatiya Thermal Power Project (O&M), Chelpur-506 170, Telangana State, India.

Article Received on 06 July 2026,
Article Revised on 27 July 2026,
Article Published on 01 August 2026,

https://doi.org/10.5281/zenodo.21772900

***Corresponding Author**

Bojja Rajeshwar Rao

Senior Chemist (Retired), Chemical Division, Kakatiya Thermal Power Project (O&M), Chelpur-506 170, Telangana State, India.

How to cite this Article: Bojja Rajeshwar Rao* (2026). Computational Study On Rna Dinucleotides Using The Am1 Semi-Empirical Method. World Journal of Pharmaceutical Research, 15(15), 1950–1964.

ABSTRACT

The thermodynamic stability, electronic structure, and global reactivity descriptors of all sixteen possible RNA dinucleotides (5′→3′: AA, AC, AG, AU, CA, CC, CG, CU, GA, GC, GG, GU, UA, UC, UG, and UU) were investigated using the semi-empirical Austin Model 1 (AM1) Hamiltonian implemented in MOPAC2016 (version 22.234w). Geometry optimisation was performed for each dinucleotide, followed by the calculation of the heat of formation, dipole moment, frontier molecular orbital (HOMO and LUMO) energies, COSMO surface area, COSMO volume, and molecular weight. Conceptual density functional theory (Conceptual DFT) global reactivity descriptors, including ionisation potential, electron affinity, electronegativity, chemical hardness, chemical softness, chemical potential, and electrophilicity index, were subsequently derived from the HOMO and LUMO energies using Koopmans' approximation. The calculated heats of formation ranged from −300.1 to −643.1 kcal mol^{-1}, indicating that all sixteen RNA dinucleotides are thermodynamically stable, with UU exhibiting the lowest heat of formation (highest thermodynamic stability) and GC the highest heat of formation (lowest thermodynamic stability). The HOMO–LUMO energy gap varied from 3.51 eV for CU to 7.73 eV for UG, suggesting that CU is the electronically softest and potentially the most chemically reactive dinucleotide, whereas UG and UU possess the greatest kinetic stability and the lowest predicted reactivity. The computed global reactivity descriptors consistently support these trends, with CU exhibiting the highest electrophilicity and lowest hardness, while UG and UU display the highest hardness and lowest electrophilicity. Overall,

this study provides a systematic quantum chemical dataset describing the thermodynamic and electronic properties of all sixteen RNA dinucleotides. These results establish a comparative reference for understanding sequence-dependent electronic behaviour and intrinsic reactivity in RNA and provide useful baseline data for future computational investigations of RNA structure, function, and molecular interactions.

KEYWORDS: RNA dinucleotides; AM1; MOPAC2016; Heat of formation; HOMO–LUMO gap; Global reactivity descriptors; Electrophilicity index; COSMO.

GRAPHICAL ABSTRACT

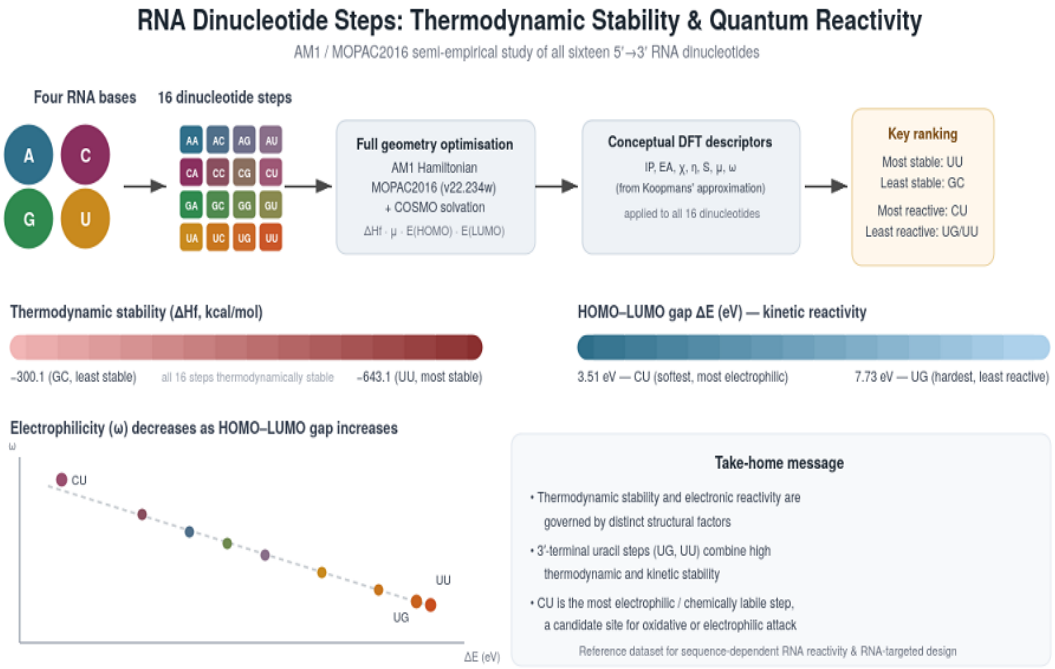

INTRODUCTION

Ribonucleic acid (RNA) plays a diverse and indispensable role in living systems, functioning as a carrier of genetic information, a catalytic molecule (ribozyme), and a regulator of gene expression. In each of these biological processes, RNA function is largely determined by the local conformational, structural, and electronic properties of its constituent dinucleotide.[1,2] The sixteen possible RNA dinucleotide combinations, formed from the four canonical ribonucleotides—adenine (A), cytosine (C), guanine (G), and uracil (U)—represent the fundamental structural and energetic units that govern RNA architecture. These dinucleotide building blocks play a crucial role in determining RNA secondary and tertiary structures through their influence on base-stacking interactions, helix formation and propagation,

conformational flexibility, and sequence-dependent stability[3]. Furthermore, the relative thermodynamic stability of individual dinucleotides affects their susceptibility to chemical modification and enzymatic recognition, thereby influencing RNA folding, biological function, and molecular interactions.

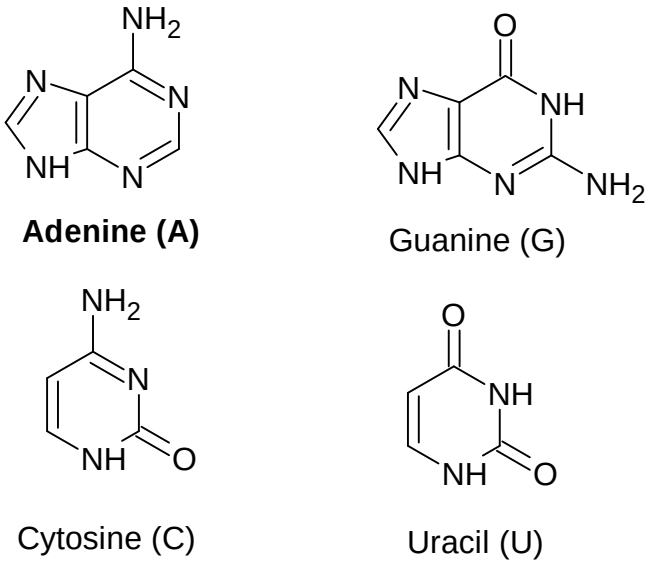

Figure 1: Four nucleobases that compose the sixteen RNA dinucleotides. Each base is linked to the ribose C1′ carbon through the labelled glyosidic bond (N9 in the purines adenine and guanine; N1 in the pyrimidines cytosine and uracil).

Quantum chemical descriptors derived from frontier molecular orbital (FMO) theory within the framework of conceptual density functional theory (DFT) have become powerful tools for understanding and predicting the chemical reactivity, stability, and site selectivity of biomolecules.[4, 5] Parameters such as the energies of the highest occupied molecular orbital (HOMO) and lowest unoccupied molecular orbital (LUMO), the HOMO–LUMO energy gap, chemical hardness (η), chemical softness (S), electronegativity (χ), chemical potential (μ), and the electrophilicity index (ω) provide quantitative measures of a molecule's resistance to charge transfer, kinetic stability, and its tendency to behave as an electrophile or nucleophile in different chemical environments.[5, 6] These global reactivity descriptors have been widely employed to investigate the physicochemical properties of small organic compounds, pharmaceuticals, and biologically active molecules. However, comprehensive computational studies that systematically correlate the thermodynamic stability and electronic reactivity of all sixteen possible RNA dinucleotides remain relatively limited. Such investigations are essential for understanding sequence-dependent variations in RNA stability, molecular recognition, and biological function at the electronic level.

In the present study, the semi-empirical Austin Model 1 (AM1)[7] Hamiltonian, implemented in MOPAC2016[8], was employed to perform complete geometry optimization of all sixteen possible RNA dinucleotides. Following optimization, key molecular properties, including the heat of formation, dipole moment, frontier molecular orbital (HOMO and LUMO) energies, COSMO-derived molecular surface area and volume[9], and molecular weight, were calculated. In continuous of research work.[10] The computed frontier orbital energies were subsequently used to derive a comprehensive set of conceptual DFT-based global reactivity descriptors.[5, 6], including the HOMO–LUMO energy gap, chemical hardness (η), chemical softness (S), electronegativity (χ), chemical potential (μ), electrophilicity index (ω), and related electronic descriptors. The primary objective of this investigation is to establish a systematic quantum chemical assessment of the relative thermodynamic stability and electronic reactivity of all sixteen RNA dinucleotides and to identify sequence-dependent trends that may provide insights into RNA structural stability, molecular recognition, and RNA-targeted chemical and biological processes. The resulting dataset offers a comprehensive framework for understanding the relationship between dinucleotide sequence, electronic structure, and molecular reactivity, thereby contributing to the broader field of RNA structural biology and computational nucleic acid chemistry.

COMPUTATIONAL DETAILS

The initial molecular geometries of all sixteen possible RNA dinucleotides (5′→3′ combinations of adenine (A), cytosine (C), guanine (G), and uracil (U)) were constructed and subjected to full geometry optimization using the semi-empirical Austin Model 1 (AM1) Hamiltonian[7] as implemented in MOPAC2016 (version 22.234w).[8] All geometry optimizations were performed without imposing any symmetry constraints, allowing each structure to relax to its lowest-energy conformation. The eigenvector-following (EF) optimization algorithm was employed until the convergence criteria based on the gradient norm were satisfied. The optimized geometries were verified to represent true local minima on the potential energy surface by confirming the absence of imaginary vibrational frequencies. To account for solvent effects, an implicit solvation model based on the Conductor-like Screening Model (COSMO)[9] was applied throughout the calculations. The COSMO approach was further used to determine the solvent-accessible molecular surface area and molecular volume of each optimized RNA dinucleotide, providing additional structural descriptors relevant to molecular interactions and solvation behavior.

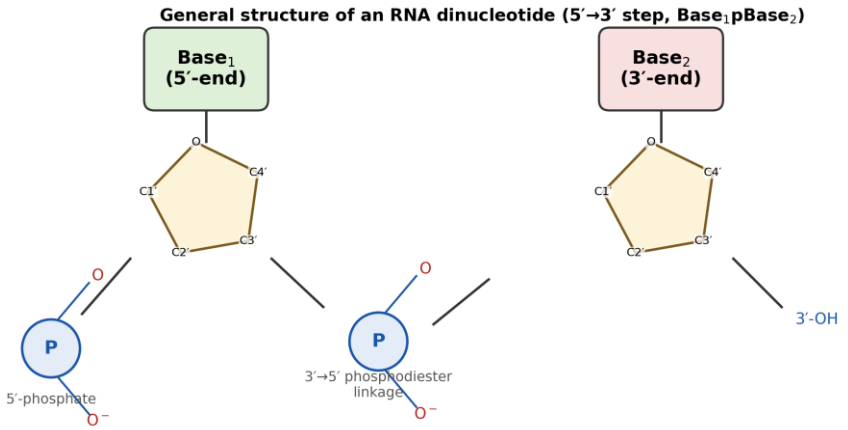

Figure 2: General repeat-unit structure of a 5′→3′ RNA dinucleotide (Base1pBase2), showing the ribose–phosphate backbone and the 3′→5′ phosphodiester linkage joining the two nucleoside units. Each of the sixteen dinucleotides modelled corresponds to a distinct Base1/Base2 combination drawn from A, C, G and U.

For each optimized RNA dinucleotide, the heat of formation (ΔHf), dipole moment (μ), and the energies of the highest occupied molecular orbital (E_{HOMO}) and the lowest unoccupied molecular orbital (E_{LUMO}) were obtained directly from the MOPAC2016 output files. These electronic properties served as the basis for evaluating the global chemical reactivity of the dinucleotides. Conceptual density functional theory (DFT)-based global reactivity descriptors were subsequently calculated from the frontier molecular orbital energies using Koopmans' theorem approximation, in which the ionization potential and electron affinity are approximated by the negative values of E_{HOMO} and E_{LUMO}, respectively. The corresponding descriptors were determined using the standard conceptual DFT equations reported in the literature.[5,6]

Ionisation potential, $IP = -E_{HOMO}$

Electron affinity, $EA = -E_{LUMO}$

HOMO–LUMO gap, $\Delta E = E_{LUMO} - E_{HOMO}$

Electronegativity, $\chi = (IP + EA)/2$

Chemical hardness, $\eta = (IP - EA)/2 = \Delta E/2$

Softness, $S = 1/\eta$

Chemical potential, $\mu = -\chi$

Electrophilicity index, $\omega = \mu^2/2\eta$

All computed values are reported in SI-consistent units (kcal/mol for energies of formation and eV for orbital-derived quantities) and are collected in Tables 1 and 2.

RESULTS AND DISCUSSION

Thermodynamic stability and molecular properties (Table - 1)

The AM1-calculated heats of formation (ΔH_f) for all sixteen RNA dinucleotides are negative, ranging from −300.12 kcal mol for GC to −643.06 kcal mol for UU (Table 1). The uniformly negative ΔH_f values indicate that all optimized dinucleotides are thermodynamically stable with respect to their constituent atoms at the AM1 level of theory. Among the sixteen dinucleotides, UU exhibits the lowest heat of formation and is therefore predicted to be the most thermodynamically stable, followed by UA (−598.25 kcal mol) and UG (−597.05 kcal mol). In contrast, GC (−300.12 kcal mol) and AA (−334.61 kcal mol) display the least negative heats of formation, indicating comparatively lower thermodynamic stability.

A clear sequence-dependent trend is observed in the calculated thermodynamic data. Dinucleotides containing uracil at the 3′ terminus (UA, UC, UG, and UU) consistently possess more negative heats of formation than their corresponding purine-terminated analogues, suggesting that uracil-containing dinucleotide steps are energetically more favorable within the AM1 computational framework. This enhanced stabilization may arise from favorable electronic interactions associated with the uracil base and its influence on the overall molecular geometry and charge distribution. Although the present calculations were performed in the gas phase with implicit solvent treatment and therefore do not explicitly account for intermolecular hydrogen bonding or crystal-packing effects, the observed trend highlights the important contribution of nucleotide sequence to the intrinsic thermodynamic stability of RNA dinucleotides. These findings provide a useful foundation for understanding sequence-dependent energetic preferences that may influence RNA folding, structural organization, and molecular recognition.

Table 1: Computed thermodynamic and structural properties of RNA dinucleotides (AM1/MOPAC2016).

RNA DI-Nucleotides	ΔHf (Kcal/mol)	Dipole (Debye)	HOMO ev	LUMO ev	Cosmo Area (sq ang)	Cosmo volume (cu ang)	Mol wt
AA	-334.6125	19.9817	-6.801	-1.809	614.27	708.66	676.4321
AC	-463.3352	6.4709	-8.857	-1.296	551.60	671.06	652.4071
AG	-400.6329	7.1669	-8.767	-1.862	651.70	736.96	692.4315
AU	-479.3431	13.6161	-6.673	-1.672	570.31	686.90	653.3919
CA	-484.5162	7.4547	-8.388	-1.603	608.71	685.49	652.4071
CC	-426.8459	11.2915	-7.356	-1.991	602.21	667.03	628.3821
CG	-407.4572	22.2023	-8.669	-2.121	633.45	709.70	668.4065
CU	-444.2462	21.9317	-6.331	-2.818	561.93	649.65	629.3669
GA	-423.0011	17.4408	-7.176	-1.997	592.11	715.85	692.4315
GC	-300.1228	10.2169	-6.950	-1.485	575.54	710.28	668.4065
GG	-458.8375	12.3383	-6.967	-1.855	587.08	724.42	708.4309
GU	-558.9861	12.4018	-8.832	-1.581	595.79	695.67	669.3913
UA	-598.2504	5.6776	-8.942	-1.439	602.06	677.26	653.3919
UC	-453.4362	23.0102	-7.582	-2.378	545.78	671.55	629.3669
UG	-597.0546	2.2208	-8.943	-1.210	601.71	701.30	669.3913
UU	-643.0568	6.6041	-9.437	-1.864	575.39	677.23	630.3517

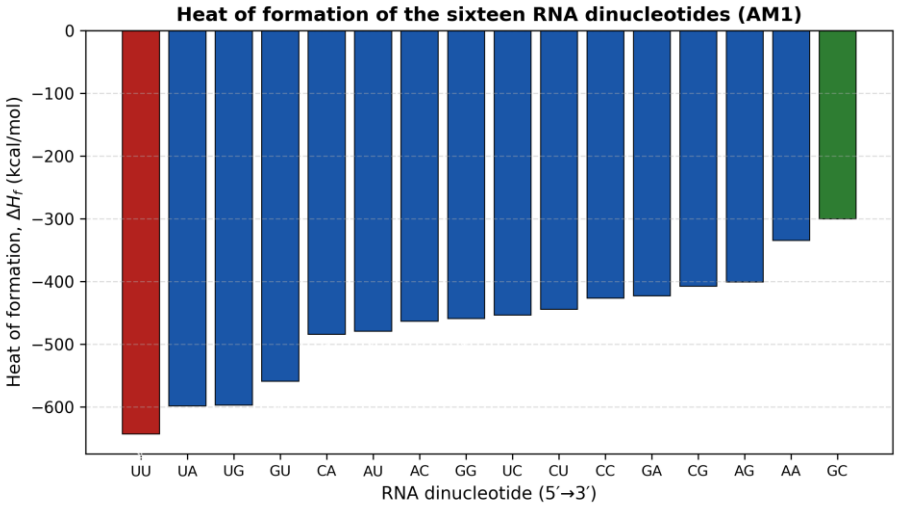

Figure 3: Heat of formation (ΔHf) of the sixteen RNA dinucleotides, ranked from most exothermic (UU, most stable) to least exothermic (GC, least stable). Red = least stable (GC); blue = most stable (UU).

The calculated dipole moments reveal substantial variation among the sixteen RNA dinucleotides, ranging from 2.22 D for UG to 23.01 D for UC (Table 1). As a measure of the overall molecular polarity, the dipole moment reflects the distribution of electronic charge within the molecule and is strongly influenced by the nucleotide sequence, relative base orientation, and conformation of the sugar–phosphate backbone. The wide range of dipole moment values observed in this study demonstrates that even subtle changes in base

composition can significantly alter the electronic polarization of RNA dinucleotides. Such differences in molecular polarity are expected to influence electrostatic interactions with the surrounding solvent, hydration behavior, counter-ion binding, and intermolecular recognition processes, all of which play important roles in RNA folding, stability, and biological function.

The structural descriptors obtained from the COSMO calculations further support the influence of nucleotide composition on molecular size. The solvent-accessible surface area varies from 546 to 652 Å², while the corresponding molecular volume ranges from 650 to 737 Å³ (Table 1). These parameters increase in parallel with molecular weight, which spans from 628 to 708 g mol, reflecting the larger atomic composition of purine-containing dinucleotides. Accordingly, purine-rich sequences such as GG and AG exhibit the largest molecular volumes, solvent-accessible surface areas, and molecular weights owing to the presence of the bicyclic purine bases, whereas pyrimidine-rich dinucleotides generally possess smaller molecular dimensions because cytosine and uracil contain single-ring heterocyclic structures. The observed relationships among molecular weight, surface area, and molecular volume are consistent with established structural characteristics of nucleic acid bases and provide additional insight into the steric and solvation properties of RNA dinucleotides.

Frontier molecular orbitals and global reactivity descriptors (Table 2)

The calculated frontier molecular orbital energies reveal significant sequence-dependent variations in the electronic structure of the sixteen RNA dinucleotides (Table 2). The energies of the highest occupied molecular orbital (E_{HOMO}) range from −6.331 eV for CU to −9.437 eV for UU, whereas the lowest unoccupied molecular orbital (E_{LUMO}) energies vary from −1.210 eV for UG to −2.818 eV for CU. These differences in frontier orbital energies reflect variations in electron-donating and electron-accepting abilities arising from changes in nucleotide composition and molecular conformation.

The corresponding HOMO–LUMO energy gap (ΔE), which is widely regarded as an indicator of kinetic stability and chemical reactivity, spans a broad range from 3.513 eV for CU to 7.733 eV for UG. Within the framework of frontier molecular orbital theory, a smaller energy gap is generally associated with greater electronic polarizability, enhanced charge-transfer capability, and increased chemical reactivity, whereas a larger energy gap indicates greater kinetic stability, lower polarizability, and reduced chemical reactivity. Based on these

results, CU is predicted to be the softest and most chemically reactive dinucleotide in the series, exhibiting the lowest kinetic stability. In contrast, UG (ΔE = 7.733 eV) and UU (ΔE = 7.573 eV) possess the largest frontier orbital energy gaps, indicating that they are electronically harder, less reactive, and kinetically more stable than the remaining dinucleotides. These sequence-dependent differences in frontier orbital energies and energy gaps suggest that the intrinsic electronic properties of RNA dinucleotides are strongly influenced by nucleotide composition and may contribute to variations in their molecular recognition, charge-transfer behavior, and structural stability.

Table 2: Global quantum chemical reactivity descriptors of RNA dinucleotides derived from HOMO/LUMO energies (AM1/MOPAC2016).

RNA DI-Nucleotides	HOMO eV	LUMO eV	ΔE eV	IP eV	EA eV	EN eV (χ)	Global Hardness eV(η)	Softness (S)	Chem Pot (μ)	Eletro-philicity Index (ω)
AA	-6.801	-1.809	-4.992	6.801	1.809	4.305	2.496	2.725	-4.305	3.713
AC	-8.857	-1.296	-7.561	8.857	1.296	5.077	3.781	2.343	-5.077	3.408
AG	-8.767	-1.862	-6.905	8.767	1.862	5.315	3.453	2.539	-5.315	4.090
AU	-6.673	-1.672	-5.001	6.673	1.672	4.173	2.501	2.669	-4.173	3.481
CA	-8.388	-1.603	-6.785	8.388	1.603	4.996	3.393	2.473	-4.996	3.678
CC	-7.356	-1.991	-5.365	7.356	1.991	4.674	2.683	2.742	-4.674	4.071
CG	-8.669	-2.121	-6.548	8.669	2.121	5.395	3.274	2.648	-5.395	4.445
CU	-6.331	-2.818	-3.513	6.331	2.818	4.575	1.757	3.604	-4.575	5.957
GA	-7.176	-1.997	-5.179	7.176	1.997	4.587	2.590	2.771	-4.587	4.062
GC	-6.950	-1.485	-5.465	6.950	1.485	4.218	2.733	2.543	-4.218	3.255
GG	-6.967	-1.855	-5.112	6.967	1.855	4.411	2.556	2.726	-4.411	3.806
GU	-8.832	-1.581	-7.251	8.832	1.581	5.207	3.626	2.436	-5.207	3.738
UA	-8.942	-1.439	-7.503	8.942	1.439	5.191	3.752	2.384	-5.191	3.591
UC	-7.582	-2.378	-5.204	7.582	2.378	4.980	2.602	2.914	-4.980	4.766
UG	-8.943	-1.210	-7.733	8.943	1.210	5.077	3.867	2.313	-5.077	3.333
UU	-9.437	-1.864	-7.573	9.437	1.864	5.651	3.787	2.492	-5.651	4.216

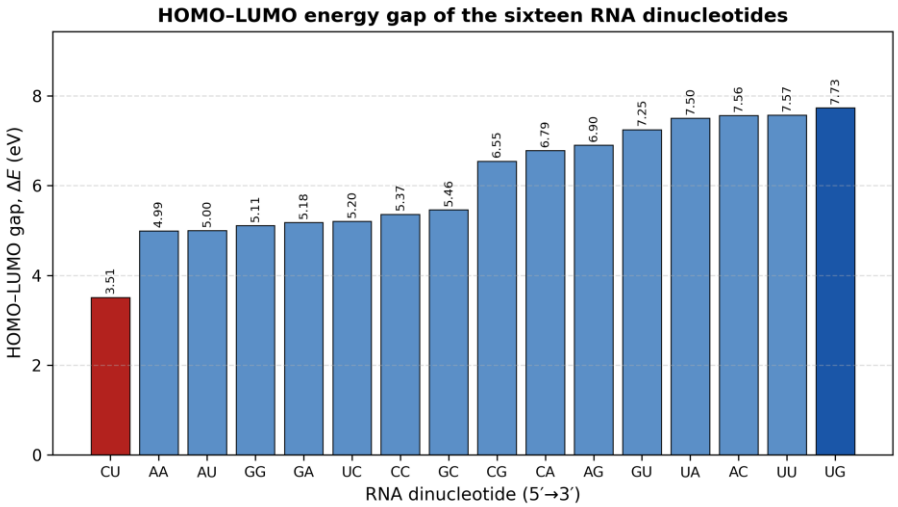

Figure 4: HOMO–LUMO energy gap (ΔE) of the sixteen RNA dinucleotides, ranked from smallest (CU, softest/most reactive) to largest (UG, hardest/least reactive).

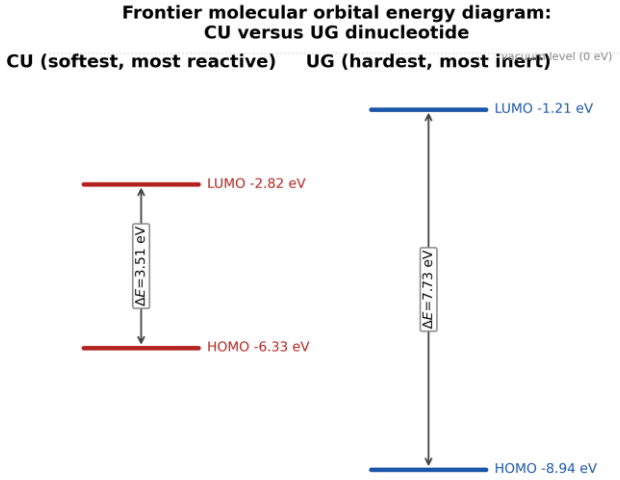

Figure 5: Frontier molecular orbital energy-level diagram comparing the two reactivity extremes of the series: CU (smallest HOMO–LUMO gap, most electrophilic) and UG (largest HOMO–LUMO gap, most chemically inert).

The sequence-dependent variation in the HOMO–LUMO energy gap is further supported by the calculated global hardness (η) and softness (S) values (Table 2). According to conceptual density functional theory, chemical hardness is a measure of a molecule's resistance to deformation of its electron cloud, whereas chemical softness reflects its ability to undergo charge transfer during chemical interactions. Consistent with its narrow HOMO–LUMO energy gap, CU exhibits the lowest chemical hardness (η = 1.757 eV) and the highest chemical softness (S = 3.604 eV^{-1}), indicating a greater propensity for electronic polarization

and enhanced chemical reactivity. In contrast, UG possesses the highest hardness (η = 3.867 eV) and the lowest softness (S = 2.313 eV^{-1}), confirming its classification as the hardest and least reactive dinucleotide in the series. These findings demonstrate the close relationship between frontier orbital energy gaps and the derived conceptual DFT descriptors, providing a consistent assessment of the relative electronic stability of the RNA dinucleotides.

The calculated ionization potential (IP) and electron affinity (EA) exhibit trends that are consistent with the frontier molecular orbital energies. As expected from Koopmans' theorem, the ionization potential follows the inverse of the HOMO energy, with UU displaying the highest IP (9.437 eV), indicating the greatest resistance to electron removal and oxidation, whereas CU has the lowest IP (6.331 eV), suggesting that it is the most readily oxidized dinucleotide. Conversely, the electron affinity is greatest for CU (2.818 eV), reflecting its strong tendency to accept an electron, while UG exhibits the lowest EA (1.210 eV), indicating the weakest electron-accepting capability. Collectively, these descriptors suggest that CU possesses the greatest susceptibility toward both electron donation and electron acceptance, characteristics that are consistent with its relatively high chemical reactivity. In contrast, the high ionization potential, low electron affinity, and large HOMO–LUMO energy gap of UG indicate a comparatively inert electronic structure with enhanced kinetic stability. These observations further emphasize the pronounced influence of nucleotide sequence on the electronic properties and reactivity of RNA dinucleotides.

The electrophilicity index (ω), which integrates chemical potential and chemical hardness to quantify the energetic stabilization of a molecule upon accepting additional electronic charge, also exhibits marked sequence-dependent variation among the sixteen RNA dinucleotides (Table 2). The highest electrophilicity index is observed for CU (ω = 5.957 eV), whereas AC possesses the lowest value (ω = 3.408 eV). The exceptionally high electrophilicity of CU, together with its small HOMO–LUMO energy gap, low chemical hardness, and high chemical softness, consistently identifies this dinucleotide as the most electrophilic and chemically reactive member of the series. Such characteristics suggest an enhanced susceptibility to charge-transfer interactions and electrophilic processes. In contrast, UG and UU, which exhibit large HOMO–LUMO energy gaps and high chemical hardness values, are predicted to be the least electrophilic and the most electronically stable dinucleotides, reflecting their comparatively inert chemical behaviour.

The calculated electronegativity (χ) and chemical potential (μ) values provide additional insight into the intrinsic electron-attracting characteristics of the RNA dinucleotides. Among the sixteen sequences, CG (χ = 5.395 eV) and UA (χ = 5.191 eV) exhibit the highest electronegativity values, indicating a greater tendency to attract electron density during chemical interactions. Correspondingly, these dinucleotides possess the most negative chemical potential values, reflecting a relatively strong thermodynamic driving force for electron acceptance. In contrast, dinucleotides with lower electronegativity values exhibit less negative chemical potentials, indicating a comparatively weaker affinity for additional electron density. Collectively, the calculated electronegativity, chemical potential, and electrophilicity descriptors demonstrate that the electronic behaviour of RNA dinucleotides is highly dependent on nucleotide sequence and complements the trends observed for frontier molecular orbital energies, chemical hardness, and chemical softness. These descriptors provide a comprehensive framework for understanding sequence-dependent differences in the chemical reactivity, charge-transfer characteristics, and electronic stability of RNA dinucleotides.

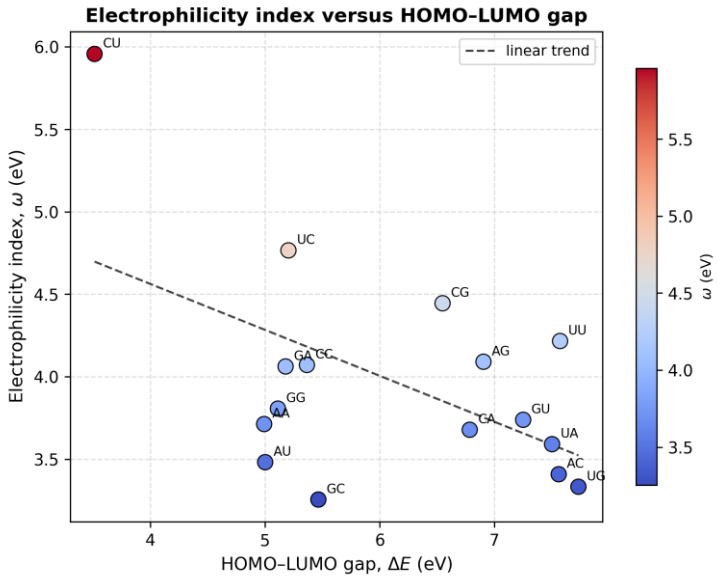

Figure 6: Electrophilicity index (ω) plotted against the HOMO–LUMO gap (ΔE) for all sixteen RNA dinucleotides, illustrating the inverse relationship between kinetic hardness and electrophilic reactivity (dashed line: linear trend).

Sequence-dependent trends

Taken together, the thermodynamic properties (Table 1) and the conceptual DFT-based quantum chemical reactivity descriptors (Table 2) provide a coherent picture of the intrinsic

stability and electronic behavior of the sixteen RNA dinucleotides. Dinucleotides terminating in uracil, particularly UG and UU, combine highly negative heats of formation with large HOMO–LUMO energy gaps, high chemical hardness, low chemical softness, and low electrophilicity indices. These complementary characteristics indicate that these sequences are both thermodynamically favorable and kinetically stable, making them the least chemically reactive members of the series. In contrast, CU exhibits the smallest HOMO–LUMO energy gap, the lowest chemical hardness, the highest chemical softness, and the largest electrophilicity index, consistently identifying it as the most chemically reactive and electronically labile dinucleotide, despite not being the least thermodynamically stable. Instead, GC and AA possess comparatively less favorable heats of formation, demonstrating that thermodynamic stability and electronic reactivity are not necessarily correlated.

The observed differences highlight the complementary nature of thermodynamic and electronic descriptors in characterizing molecular behavior. Whereas the heat of formation primarily reflects the overall energetic stability arising from molecular bonding, geometry, and steric and electrostatic interactions, frontier molecular orbital energies and their derived conceptual DFT descriptors describe the ease of electron transfer, charge redistribution, and chemical response to external perturbations. Consequently, molecules with high thermodynamic stability are not invariably the least reactive, and relatively less stable molecules are not necessarily the most reactive. The sequence-dependent trends identified in the present study therefore provide a quantitative framework for understanding how nucleotide composition influences both the intrinsic stability and electronic properties of RNA dinucleotides. These findings may contribute to predicting sequence-dependent differences in molecular recognition, charge-transfer behavior, and susceptibility to oxidative or electrophilic reactions, thereby offering useful insights into RNA structural biology, nucleic acid chemistry, and the rational design of RNA-targeted therapeutic and biochemical studies.

CONCLUSIONS

The present AM1 semi-empirical quantum chemical investigation provides a comprehensive evaluation of the thermodynamic stability and electronic reactivity of all sixteen possible RNA dinucleotides. The calculated heats of formation indicate that all dinucleotides are thermodynamically stable at the AM1 level of theory, with UU exhibiting the greatest thermodynamic stability and GC the lowest. Analysis of the frontier molecular orbitals and

the derived conceptual DFT-based global reactivity descriptors demonstrates pronounced sequence-dependent variations in electronic properties. Among the sixteen dinucleotides, CU is characterized by the smallest HOMO–LUMO energy gap, the lowest chemical hardness, the highest chemical softness, and the greatest electrophilicity index, identifying it as the most electronically reactive and chemically labile sequence. In contrast, UG and UU possess the largest HOMO–LUMO energy gaps, the highest chemical hardness, and the lowest electrophilicity, indicating enhanced kinetic stability and comparatively inert electronic behaviour.

Overall, the calculated thermodynamic and quantum chemical descriptors provide a systematic framework for comparing the intrinsic stability and reactivity of RNA dinucleotide steps. The observed sequence-dependent trends demonstrate that thermodynamic stability and electronic reactivity are complementary but distinct molecular properties, each contributing unique insights into RNA behavior. These results establish a valuable computational reference for future investigations of RNA structure–property relationships, sequence-dependent charge-transfer processes, and molecular recognition. Furthermore, the dataset may support the interpretation of RNA chemical reactivity, guide the design of RNA-targeted therapeutic agents, and provide a foundation for higher-level quantum chemical and molecular simulation studies aimed at understanding the structural and functional properties of RNA.

ACKNOWLEDGEMENT

The author is gratefully acknowledges Dr. D. Rajendra Prasad (Retired), Professor of Education, Kakatiya University, India for giving the critical suggestions to carry out this work. The author also acknowledges the use of artificial intelligence (AI)-based language assistance, including both Claude AI and ChatGPT, during the preparation and editing of the manuscript. The author takes full responsibility for the accuracy, interpretation, and final content of the article.

Disclosure statement

No potential conflict of interest was reported by the author.

Funding

The author received no financial support for the research work, and publication of this article.

Author's contribution

The author has participated in conception, design, analysis, interpretation of the data, drafting the article, and approval of the final version.

REFERENCES

1. Saenger W, Principreles of Nucleic Acid Structure (Springer-Verlag, New York), 1984. https://doi.org/10.1007/978-1-4612-5190-3
2. Bloomfield V A, Crothers D M & Tinoco I, Nucleic Acids: Structures, Properties, and Functions (University Science Books, Sausalito, CA), 2000. https://www.worldcat.org/isbn/9780935702491
3. SantaLucia J Jr, Proc Natl Acad Sci USA, 1998; 95: 1460. https://doi.org/10.1073/pnas.95.4.1460
4. Parr R G & Yang W, Density Functional Theory of Atoms and Molecules (Oxford University Press, New York), 1989. https://global.oup.com/academic/product/density-functional-theory-of-atoms-and-molecules-9780195092769
5. Parr R G & Pearson R G, J Am Chem Soc, 1983; 105: 7512. https://doi.org/10.1021/ja00364a005
6. Parr R G, Szentpaly L V & Liu S, J Am Chem Soc, 1999; 121: 1922. https://doi.org/10.1021/ja983494x
7. Dewar M J S, Zoebisch E G, Healy E F & Stewart J J P, J Am Chem Soc, 1985; 107: 3902. https://doi.org/10.1021/ja00299a024
8. Stewart J J P, MOPAC2016 (Stewart Computational Chemistry, Colorado Springs, CO, USA), 2016. http://openmopac.net/
9. Klamt A & Schuurmann G, J Chem Soc Perkin Trans, 1993; 2: 799. https://doi.org/10.1039/P29930000799
10. Rajeshwar Rao B, Computational study of the thermodynamic properties of nucleosides in ribonucleic acid (RNA) using the Austin Model-1 Method, *World J Pharmaceutical Research*, **2025;** 14(13): 259-274. www.wjpr.net